

NEAR FIELD GROUND MOTION.

V.V.Shteinberg^I, Yu.K.Chernov^{II}, T.G.Ivanova^{III}.

SUMMARY.

The near field and far field zones are distinguished on the basis of analysis of displacement and acceleration records. The different correlations of ground vibration parameters with magnitude and focal distances are observed in these zones. The principle opportunity of strong motion estimation on the basis of small earthquake records analysis from the same tectonic region is shown.

INTRODUCTION.

Quantitative correlations of peak acceleration and displacement, periods and spectra with earthquake magnitude and focal distances are considered in this report. About 100 records of strong earthquakes ($M_L=4.5-7.6$) recorded in the USA, Japan, and Europe were used for the analysis. The aftershock records from Gazli, USSR of 1976, $M_L=7.3$ (about 500 records) and San-Fernando, USA of 1971, $M_L=6.4$ (200 records) have been used too.

GROUND ACCELERATION AND DISPLACEMENT.

Fig.I shows displacements (left column) and accelerations (right column) for some Gazli aftershocks simultaneously recorded by C5C seismometer ($T_s=0.05$ sec) installed on the surface of thick (1400 meters) sandy-clay deposit (I,2). The 75% of horizontal displacement records have rather a simple shape of one-sided impulse accompanied by a small oscillations. These records were obtained at short focal distances equal and less than 3-5 length of the source. It was determined that the main phase of ground displacement was caused by shear wave excited by the fault displacement of "ramp" time function type. At a long distance the displacement records got complicated by converted and surface waves when the "degeneration" of the main impulse occurred. The complication of record occur by increasing the source size. For instance, the seismograms of Gazli and San-Fernando main shocks consist of several strong and rather long period ($T = 3-6$ sec) oscillations. By the comparison the acceleration with displacement it's noted the existence of different shape of accelerations by the likeness of displacement records (see Fig.I). In Gazli tectonic zone the different type of acceleration records were obtained at the same site as a result of the earthquakes with the same source mechanism, magnitude and depth. So, the conclusion about connection the main phase of displacement with general fault movement can be drawn. On the contrary the short wave radiati-

I. Chief of Laboratory, Institute of Physics of the Earth, Moscow, USSR.

II. Minor scientist, Institute of Seismology, Tashkent, USSR.

III. Minor scientist, Institute of Physics of the Earth, Moscow USSR.

on by the large earthquake is connected with some peculiarities of fault propagation.

Validity of this conclusion is confirmed by experiments with pre-existing shear cracks in the laboratory (3). The increasing of short period radiation energy is observed by the simulation of local inhomogeneities in the crack surface (cemented points). The pulse shape was not stable varying from experiment to experiment. Therefore, the correlation of short period vibration parameters with earthquake magnitude and distances must be accompanied by a large scattering.

Fig.2 shows the graph of the peak accelerations dependence a_{max} on epicentral distances Δ for different earthquake magnitude M (4). Every curve $a_{max} = f(\Delta)$ is envelope of a number of individual points. Some individual extremely large values haven't been taken into account when drawing the curves. Site conditions weren't taken into consideration. The graph of dependence can be divided into two parts concerning near field (N.F.) and far field (F.F.) zones. The value of epicentral distance Δ_0 approximately equal to the length of the fault is a boundary of N.F. zone. The poor correlation of peak acceleration with distances and earthquake magnitude (when $M \geq 6.0$) were determined. In F.F. zone when $\Delta > \Delta_0$ the peak acceleration decreases inversely proportional to Δ^6 . The values a_{max} , Δ_0 and "8" are given in Table I.

The lack of correlation of period T of peak acceleration with distance is observed in N.F. zone. The weak dependence of period on magnitude was observed (5)

$$\lg T_{sec} = 0.18 M_L - 1.6 \quad (1)$$

The relationships between spectral amplitude S_a , frequency f_{max} of maximum of smoothed Fourier amplitude spectra and M are shown in the following formulas

$$d \lg S_a / d M = 0.56 \quad (2)$$

N.F. zone

$$\lg f_{max} = 1.6 - 0.2 M \quad (3)$$

$$d \lg S_a / d M = 0.63 \quad (4)$$

F.F. zone

Fig.3 shows a strongly smoothed response acceleration spectra (damping - 0.05) for N.F. zone. The dependence of spectral amplitudes \ddot{Y} , period of spectral maxima T on M are given in the following equations

$$\lg \ddot{Y}_{sm.sec^{-2}} = 0.25 M + 1.4 \quad (5)$$

$$\lg T_{sec} = 0.09 - 1.1 \quad (6)$$

for N.F. zone and

$$\lg \ddot{Y}_{sm.sec^{-2}} = 0.25 M + 1.3 \quad (7)$$

$$\lg T_{\text{sec}} = 0.12 M - 1.2 \quad (8)$$

for F.F. zone.

On the contrary the independence of peak acceleration on magnitude in N.F. zone, the increasing of spectral amplitude can be explained by increasing seismic signal duration when the length and width of the fault is enlarged.

The dependence of peak displacement on focal distance R and magnitude M is illustrated in Fig.4. The seismograms of Gazli aftershocks with $M_L = 2.7 - 5.5$ were used for the analysis. The solid lines in this figure show the regression trend of peak values A (in millimeters) for $R = 3 - 400$ km. Two segments of every curve corresponding to N.F. zones could be distinguished. In N.F. zone the amplitude and period of displacement weakly depend on distance. But A and T depend on earthquake magnitude

$$\lg A_{\text{mm}} = 0.53 M - 1.41 \quad (9)$$

$$\lg T_{\text{sec}} = 0.21 M - 1.57 \quad (10)$$

For F.F. zone equation can be written as

$$\lg A_{\text{mm}} = (0.1 M - 2.09) \lg R_{\text{km}} + (0.96 M - 2.07) \quad (11)$$

$$\lg T_{\text{sec}} = 0.28 M + 0.13 \lg R_{\text{km}} - 1.54 \quad (12)$$

For Sa-Fernando earthquakes with $M = 1.5 - 4.5$ in N.F. zone

$$\lg A_{\text{mm}} = 0.48 M - 2.0 \quad (13)$$

$$\lg T_{\text{sec}} = 0.42 M - 1.92 \quad (14)$$

Thus, the displacement is more sensitive with magnitude changing than acceleration.

By the estimating the length of N.F. zone, the errors δR of focal coordinates calculation must be taken into account. At the expense of these errors the real length L of N.F. zone can be increased up to $L + 2\delta R$.

The calculation of strong displacements was carried out on the basis of equations (9) - (14). The dashed lines in Fig.4 are calculated curves. Upper calculated curve corresponds to attenuation curve for the earthquake with $M = 7.3$. Crosses and circles are available amplitude data which obtained by the main shocks of Gazli earthquakes ($M = 7.3$; $M = 7.0$). Thick solid and dotted lines are real and calculated attenuation curves for main shock of San-Fernando earthquake ($M_0 = 6.4$). The calculated and real values are in good agreement.

The dependence of displacement Fourier spectra on M and R is determined by using of 260 spectra of Gazli earthquakes and about 200 spectra of San-Fernando aftershocks. Near field and far field zones are distinguished too. The dependence $S_d = f(M, R)$ can be described by coefficients $n = d \lg S_d / d \lg R$ and $\beta = d \lg S_d / d M$ (6). In N.F. zone spectral amplitude doesn't depend on distance. For F.F. zone

$$n = -0.65 \lg f - 1.6 \quad \text{Gazli zone} \quad (I5)$$

$$n = -0.68 \lg f - 1.7 \quad \text{San-Fern.zone} \quad (I6)$$

when the $f > f_c$; f_c - corner frequency. The increasing of n by decreasing of frequency is observed for $f < f_c$. The coefficient β depends on frequency.

For N.F.zone in Gazli and San-Fernando

$$\beta \begin{cases} = \text{const} & f < f_c \\ = -0.46 \lg f + 0.64 & f \geq f_c \end{cases} \quad (I7)$$

Thus, the dependence spectra on magnitude^c and Focal distance in N.F.zone is similar for Gazli and San-Fernando thrust Faulting earthquakes. In F.F.zone the dependence is different because of different geological structure.

Fig.5 shows the average spectral curves of Gazli after-shocks ($M = 2.7 - 5.0$), when $R \leq 15$ km. The displacement spectrum of the Gazli main shock was calculated by using relationships (I5)-(I7). Real and predicted spectral curves are shown in Fig.5 by solid and dashed lines.

CONCLUSIONS.

The correlation of peak acceleration and displacement, periods and spectra with earthquake magnitude and focal distance are determined. The near field and far field zone are distinguished. An attempt has been made to calculate strong ground motion on the basis of analysis of small earthquakes records at the same tectonic zone. The predicted values are good agreement with available Gazli and San-Fernando strong motion data. The results can be explained by the peculiarities of short waves radiation from extended fault.

REFERENCES.

1. Aptekman J., Graizer V., Pletnev K. et al. Some Data About Processes in Gazli Earthquake Epicentral Zone of 1976. Proceed.Inst.Phys.of the Earth."Eng. Seism.Probl." v.I9, Moscow, Nauka, 1978, pp149-166.
2. The Instruments and Methods of Seismometrical Observation in the USSR. Moscow, Nauka, 1974, 154 pp.
3. Vinogradov S. Experimental Observations of Elastic Wave Radiation Characteristics from Tensile Cracks and Pre-existing Shear Faults. Pageoph. v.II6, Birkhauser Verlag Basel, 1978, pp.888-899.
4. Kraminin P., Shteinberg V. The parameters of solid ground vibration by the strong earthquakes. Essay information. Series XIV N 3, Moscow, 1975, pp.55-58.
5. Aptikaev F., Gladisheva G., Iton J. et al. The connection between parameters of ground vibration by the strong and weak earthquakes. Trans. of soviet-american investigation on earthquake prediction. v.2.p.2. Dushanbe-Moscow, Donish, 1979,

pp.280-288.
 6.Khalturin V., Rautian T. The dependence of seismic spectrum on earthquake energy. Proc.3 Europ.Symp. Earth.Eng.Sofia,1970,pp.I09-II4.

Table I

parameter	M_L			
	5.5	6.0	6.5	7.5
α_{Δ}^{max} , $sm \cdot sec^{-2}$	400	500	550	600
Δ , km	10-12	15-20	25-30	40-50
β	2.2	1.9	1.75	1.7

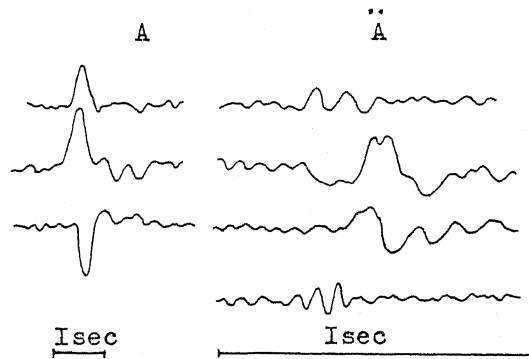
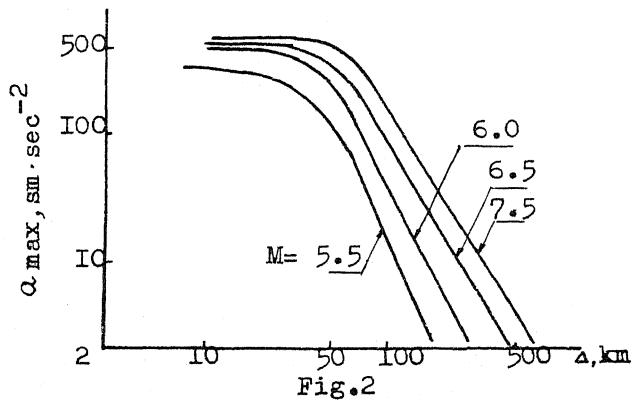


Fig.1



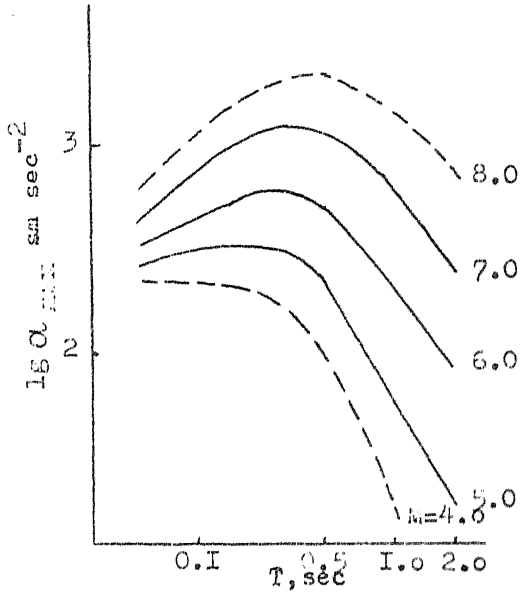


Fig. 3

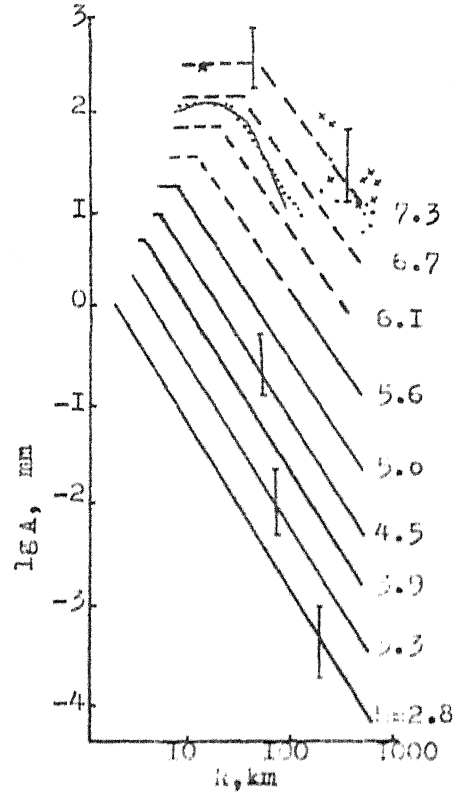


Fig. 4

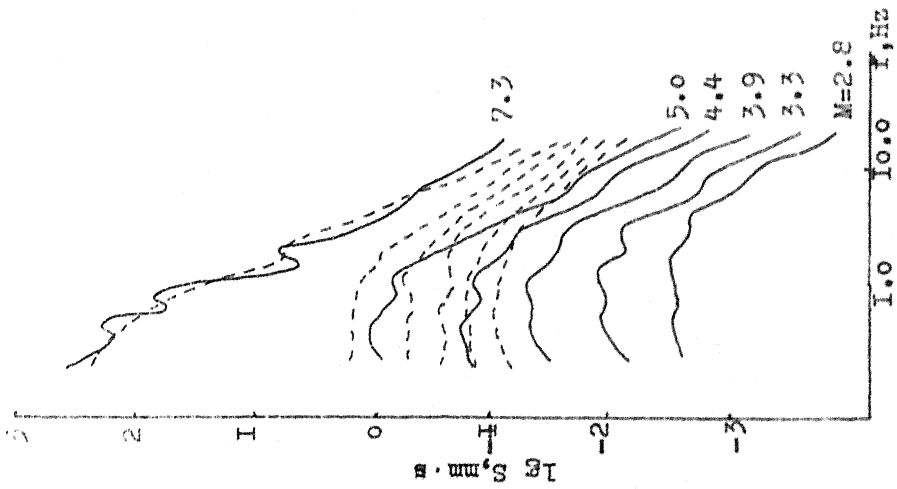


Fig. 5